

# Green Synthesis and Characterization of Silver-Copper Bimetallic Nanoparticles Using *Alternanthera brasiliana* Stem Extract

## ABSTRACT

The green synthesis of bimetallic silver copper nanoparticles (Ag-CuNPs) has gained attention due to their broad applications. Here, Ag-Cu bimetallic nanoparticles were synthesized using an aqueous extract from the stem of *Alternanthera brasiliana*. The phytochemical composition of the extract was evaluated through standard phytochemical tests, and the formation of nanoparticles was tracked using UV-visible spectroscopy. The resulting nanoparticles were further characterized using Fourier Transform Infrared (FTIR) spectroscopy, and X-ray diffraction (XRD). Using the Debye-Scherrer formula to interpret XRD data, the estimated sizes of the silver, copper, and silver-copper nanoparticles were 11.81 nm, 55.33 nm, and 12.45 nm, respectively, all synthesized under comparable conditions. Additionally, the antimicrobial properties of these nanoparticles were evaluated, revealing significant activity against various selected microorganisms. The study highlights an eco-friendly approach for synthesizing Ag-CuNPs with promising antimicrobial potential.

**Keywords:** *Alternanthera brasiliana*, green synthesis, Ag-CuNPs, XRD, antimicrobial activity

## 1. INTRODUCTION

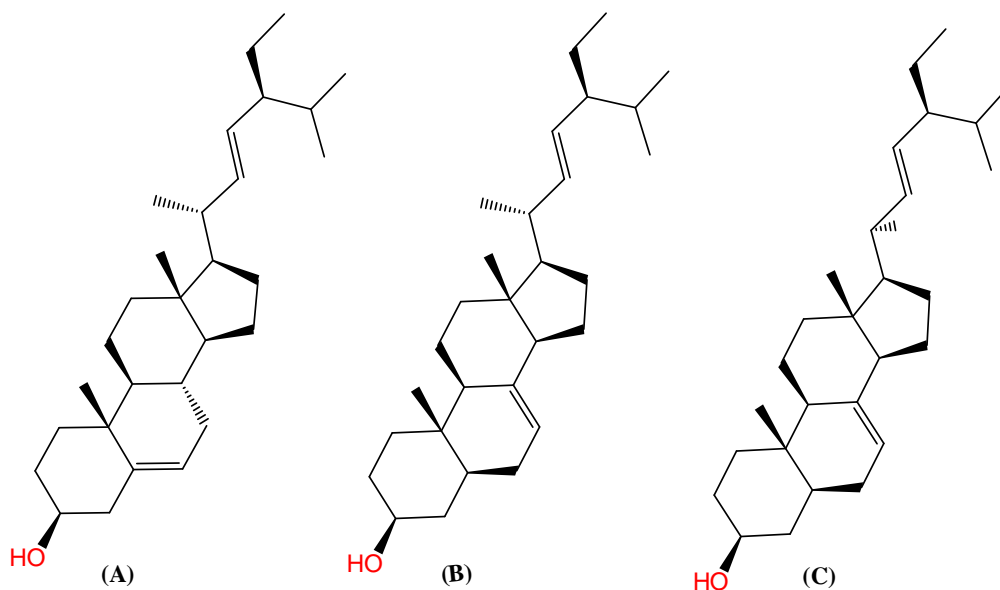
Nanoparticles have idiosyncratic properties due to profound surface-to-volume ratio and peculiar quantum confinement [1, 2]. These captivating activities have led to their applications in various fields such as medicine, pharmaceuticals, drug delivery, antifungal and antibacterial, etc. [3]. The synthesis of metal and metal oxide nanoparticles for targeted applications is in focus. Synthesis of silver and copper nanoparticles has raised attention over the last decade because of the low cost and great applications in optical, heat systems, catalysts, and sensor properties, and also as an antimicrobial agent [4- 6]. Nanoparticles can be synthesized by various methods among which the green technique is most preferred [4, 7]. Preference for the green synthesis method is due to its eco-friendliness, less expensive, and free from toxic contaminants [8]. Herein, the non-toxic, easily available, and abundant phytochemical constituents such as alkaloids, flavonoids, terpenoids, saponins, tannins, etc. are used to reduce the metal ions and stabilize the nanoparticles [9, 10]. The use of phyto-constituents is being greatly popularized nowadays as these offer advantages like antibacterial, natural reducing, and stabilizing capabilities [11, 12].

Silver nanoparticles have been synthesized using *Zingiber officinale* leaves extract [13], *Capsicum annum* [14], *Azadirachta indica* [15], and *Jatropha curcas* [16] with good antimicrobial activities. Copper nanoparticles synthesized using *Zingiber officinale* rhizome [9], *Citrus medica* [17], *Citrus limon* [18], and *Azadirachta indica* [19] with good antimicrobial activities have been reported. Bimetallic nanoparticles can be synthesized in a non-hazardous, economical, and easy way using phytochemicals [20]. Some researchers have synthesized the Ag-Cu bimetallic nanoparticles using *Phoenix dactylifera* leaves and studied their catalytic and antibacterial activities [21], using *Trigolella foenum* [22], using *Curcuma longa* for the reduction of persistent organic pollutants [23], and *Aerva lanata* extract and evaluate their cytotoxic and antimicrobial activities [24]. Bimetallic nanoparticles have a diverse range of applications across electrical, optical, catalytic, and biomedical fields [20]. It is understood that charge transfer between metal ions can catalyze various chemical reactions. Furthermore, bimetallic nanoparticles exhibit significant potential in nanomedicine and other biomedical applications [25-27]. An example of this is Cu-Fe bimetallic nanoparticles, which have been reported to effectively remediate environmental issues, particularly in removing nitrates from groundwater [28]. Ag-Cu bimetallic nanoparticles synthesized by using *Phoenix dactylifera* leaf extract have shown excellent photocatalytic activity to degrade the methylene blue dye from wastewater [29]. In addition, bimetallic nanoparticles can function as antimicrobial agents in conjunction with bacteria [30]. These nanoparticles disrupt bacterial growth by destabilizing their membranes and generating reactive oxygen species (ROS), which cause DNA damage and interfere with protein function [18,31,32]. Notably, Ag-Cu bimetallic nanoparticles have shown remarkable antimicrobial activity against Gram-positive bacteria [33]. Some pieces of literature have shown the synthesis of Ag-Cu bimetallic nanoparticles. However, Nonetheless, different plants contain different phytochemicals and they have different capacities for the reduction of metal ions and stabilization of nanoparticles [34]. Based on the literature, synthesis of Ag-Cu bimetallic nanoparticles using *Alternanthera brasiliana*

44 extract has not been conducted. *Alternanthera brasiliana* is a native Nepalese perennial herb planted for ornamental as  
45 well as traditional medicinal value points (Figure 1). Stigmasterol, spinasterol, and  $\beta$ -sitosterol as shown in scheme 1 are  
46 the reported phytosterol compounds of this plant [35].



47  
48 **Fig. 1. Vegetative part of the plant**



49  
50 **Scheme 1: Structural formula of (A) Stigmasterol, (B) Spinasterol, and (C) Beta-sitosterol**

## 51 2. MATERIALS AND METHODS

### 52 2.1 Collection of Plant material and Preparation of Extract

54 *Alternanthera brasiliana* stems sample was collected from the Nawalpur District (27°31' N, 83°39'E), Nepal. The sample  
55 was washed with tap water followed by distilled water. It was dried for 15 days and converted into fine pieces. Those  
56 pieces were crushed into fine powders with the help of an herbal disintegrator. An aqueous extract was prepared by  
57 immersing 10 g of powdered material in 150 mL of distilled water for 24 hours. The solution was filtered to obtain the  
58 aqueous extract, which was then used as a reducing and stabilizing agent in nanoparticle synthesis. The possible  
59 phytochemicals (responsible for reducing and stabilizing nanoparticles) present in aqueous extract were confirmed by  
60 respective chemical test methods.

### 61 2.2 Synthesis of nanoparticles

62 Silver nanoparticles (AgNPs) were synthesized by stirring a mixture of 20 mL precursor solution (0.1N AgNO<sub>3</sub>), 60 mL of  
63 aqueous extract, and 30 mL of distilled water in a beaker for 40 minutes. The colloid particles produced were centrifuged  
64 and collected in a watch glass. The collected mass was washed with ethanol repeatedly to remove the impurities and then

the collected mass was dried. Triplicate experiments for synthesis followed by centrifugation-decantation-washing processes were carried out and the obtained residue was dried and labeled as AgNPs. A similar process was used to synthesize copper nanoparticles (CuNPs) only using 0.1N Cu(NO<sub>3</sub>)<sub>2</sub> as the precursor solution instead of the silver precursor solution. Likewise, silver-copper bimetallic nanoparticles were synthesized using 20 mL of 0.1N AgNO<sub>3</sub> and 20 mL of 0.1N Cu(NO<sub>3</sub>)<sub>2</sub> mixture as precursor solution, 60 mL of aqueous extract, and 30 mL of distilled water. All synthesis protocols and environments were constant with the AgNPs synthesis process. The dry mass collected was labeled as Ag-CuNPs.

## 2.3 Nanoparticle Characterization

The formation of nanoparticles in the colloidal form in the reaction mixture was monitored using UV–Visible double-beam spectrometer (2802LT, Labtronics). The sample solution in the cuvette was irradiated with electromagnetic radiation of wavelength 200 to 800 nm and the absorbance was recorded. Similarly, the functional groups of AE associated with stabilizing the nanoparticles were identified using Fourier transform infrared (FT-IR) spectroscopy. Solid nanoparticle samples were scanned in the range 4000-400 cm<sup>-1</sup> with a scan interval of 4 cm<sup>-1</sup> using a Perkin Elmer 10.6.2 spectrometer at the Department of Chemistry, Amrit Campus, and Kathmandu. The crystallinity of the synthesized nanoparticles was determined using an X-ray diffractometer (Rigaku-D/max 2500 PC diffractometer). Nanoparticles were exposed to incident X-rays (CuK<sub>α</sub>, 1.5406 Å) at a scanning rate of 10°/min from a 10-90° angle and the intensities of diffracted rays at 2θ angle were recorded. The inter-planar spacing, crystal planes, and grain size of the nanoparticles were calculated using Bragg's equation (1) and Debye Sherrer's formula (2), as below [18,36].

$$n\lambda = 2d \sin \theta \quad (1)$$

$$\text{Grain Size (D)} = k \lambda / \beta \cos \theta \quad (2)$$

Where, D = grain size, d = inter-planar distance, λ = 1.5406 Å (wavelength of X-ray used), K = constant (equal to 0.94 for cubic crystal system), θ = diffracted angle, β = Full width at half maximum in radian.

## 3. RESULTS AND DISCUSSION

### 3.1 Phytochemical test results

Phytochemicals are the potential reducing and stabilizing agents. To ensure the possible reducing and stabilizing agents, the phytochemical screening of aqueous extract of *Alternanthera brasiliana* stem was performed, and the findings are tabulated in Table 1.

**Table 1. Phytochemicals present in the aqueous extract of *Alternanthera brasiliana* stem**

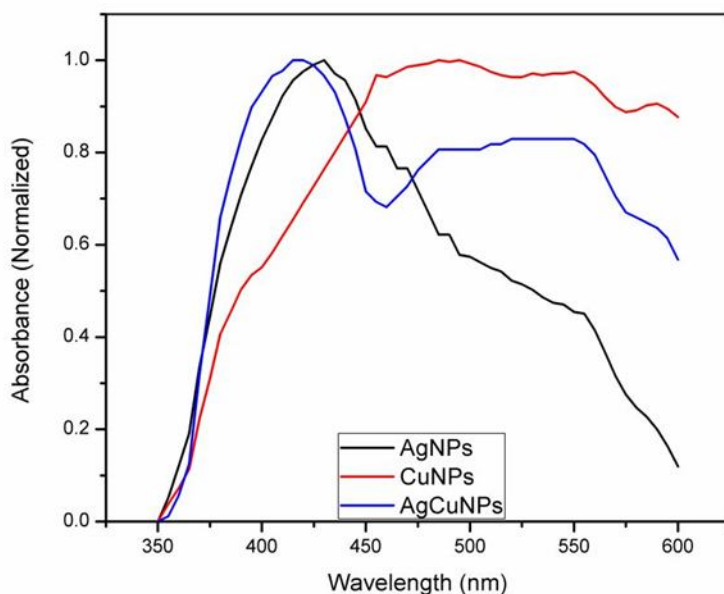
S.N.	Phytochemicals	Aqueous Extract
1	Alkaloids	+
2	Flavonoids	-
3	Carbohydrates	+
4	Phenol and Tannins	+
5	Quinones	-
6	Proteins	-
7	Saponins	+
8	Terpenoids	+
9	Glycosides	-
10	Fat and Oils	+

Absence (-), Presence (+)

### 3.2 UV Spectra Analysis

UV absorbance spectra of synthesized nanoparticles obtained due to surface Plasmon resonance with incident UV wave are shown in Figure 2. The maximum absorbance at 425 nm indicated the formation of AgNPs. Similar findings were reported by Tamarasi and co-workers in which the maximum absorption peak was observed around (425 nm) [37]. Similarly, the maximum absorbance at 487 nm indicated the formation of CuNPs. Similar findings were reported by Sowbaraniya and co-workers in which the maximum absorption peak was observed at 480-515 nm [38]. Likewise, the maximum absorbance at 412 nm indicates the formation of Ag-Cu NPs. The UV spectral lines due to the surface Plasmon

103 resonance of the bimetallic nanoparticle are broad in comparison to individual nanoparticles. This implies that the  
104 bimetallic nanoparticle showed an effect for broad spectrum indicating the broad spectrum interaction with the light.



105  
106 **Fig. 2. Combined UV spectra of AgNPs, CuNPs, and AgCuNPs**

### 107 3.3 FT-IR Spectra Analysis

108 FTIR spectroscopy is a powerful tool for the identification of functional groups. Herein, the functional group associated  
109 with capping and stabilizing nanoparticles was identified using this tool. Not all but the majority of the functional groups of  
110 AE may be oxidized thereby reducing metal ions to metal nanoparticles. Those oxidized as well as non-oxidized functional  
111 groups may be responsible for the stabilization of Ag NPs, Cu NPs, and Ag-Cu NPs nanoparticles. The main functional  
112 groups that are associated with stabilizing the AgNPs are O-H, C=C, and C=C conjugated amide groups of C-H showing  
113 stretching and bending vibrations at 3475, 3038, 2512, and 796  $\text{cm}^{-1}$  respectively [11,36,39]. The main functional groups  
114 that are associated with stabilizing the copper nanoparticles are O-H, C-H, and  $\text{CH}_2$  stretching aliphatic groups, C=C  
115 conjugated and alkene of C-H showing stretching and bending vibrations at 3403, 2956, 2708, 2566, and 2356  $\text{cm}^{-1}$   
116 respectively [9,39]. Likewise, the main functional groups that are associated to stabilize the silver-copper bimetallic  
117 nanoparticles are O-H, C-H, and  $\text{CH}_2$  stretching aliphatic groups, C=O group of quinone compounds, C=O carbohydrate,  
118 aromatic compound, halogen compound (iodo compounds) showing stretching and bending vibrations at 3409, 2888,  
119 1669, 1078, 827 and 626  $\text{cm}^{-1}$  [20,39-41]. From Figure 3, it was clear that almost all the functional groups for the reduction  
120 and stabilization of these three nanoparticles are the same. It is evident that -OH, -CH, -C=O, C-N, and NH functional  
121 groups are the major groups for the stabilization of nanoparticles.

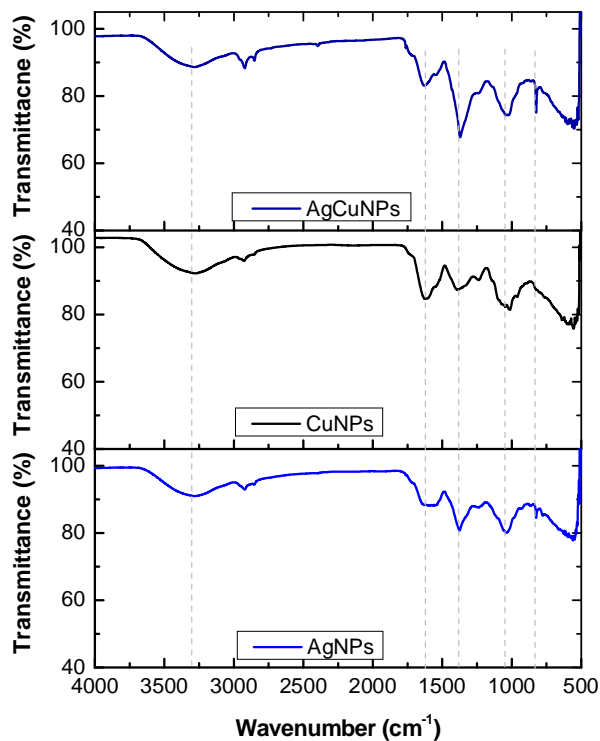


Fig. 3. Combined FTIR spectra of AgNPs, CuNPs, and Ag-CuNPs

### 3.4 XRD Spectra Analysis

XRD patterns obtained for AgNPs, CuNPs, and Ag-CuNPs are shown in Figure 4. The diffraction peaks at  $2\theta$  value were observed at 27.66, 32.16, 38.15, 46.14, 54.56, 57.28, 65.5, 76.6 and 85.16 for AgNPs (Figure 4(a)). Diffraction peaks at 38.15, 65.5, and 76.6 are (111), (220), (311) crystalline plane of AgNPs (JCPDS No. 04-0783) whereas diffraction peaks at 27.66, 32.16, 46.14, 54.56, 57.28, and 85.16 are (110), (111), (200), (220) and (222) crystalline planes of AgONPs (JCPDS No. 43-0997 and JCPDS No. 43-1038). These oxide peaks may be due to the surface aerial oxidation of nanoparticles. However, Mehta and co-workers reported the crystalline patterns for AgNPs are at 32.35, 46.38, 54.03, and 57.66 [42], and also similar findings are reported by Giri and co-workers for AgNPs [43]. The XRD pattern confirmed that the synthesized AgNPs are a face-centered cubic crystal structure.

The diffraction peaks ( $2\theta$  values) for CuNPs were observed at 43.06 and 53.36 as shown in Figure 4(b). The diffraction peak at 43.06 and 53.36 have phases of (111) and (220) plane systems (JCPDS No. 04-0836). Similar findings were reported for green synthesized CuNPs in which diffraction peaks were observed at 43.26, 50.32, and 74.05 degrees which indicated the formation of Cu nanoparticles [9, 18, 44]. The sharp peaks of the XRD pattern indicated the crystalline nature of CuNPs. XRD pattern of bimetallic Ag-CuNPs showed diffraction peaks ( $2\theta$  values) at 28.08, 32.14, 38.15, 43.06, 46.14, 54.6, 57.28, 65.58, 76.6 and 85.16 as shown in figure 4(c) (JCPDS No. 04-0783 and JCPDS No. 04-0836). These  $2\theta$  values completely resemble the diffraction angles as shown by AgNPs and CuNPs individually. The diffraction pattern shown by these bimetallic nanoparticles indicates the formation of bimetallic Ag-CuNPs. Rahman and co-workers reported similar findings in which the fcc structure of Ag-CuNPs was validated by five characteristic peaks corresponding to the (111), (200), (220), (222), and (311) planes that occurred at 18, 36, 42, 60, and 64, respectively [45].

The detailed peak position, their miller indices, and the crystal structure for all nanoparticles are shown in Table 2. Similarly, the average grain size determined by applying the most intense peak width (FWHM) in the Debye Scherer's formula is given in Table 3.

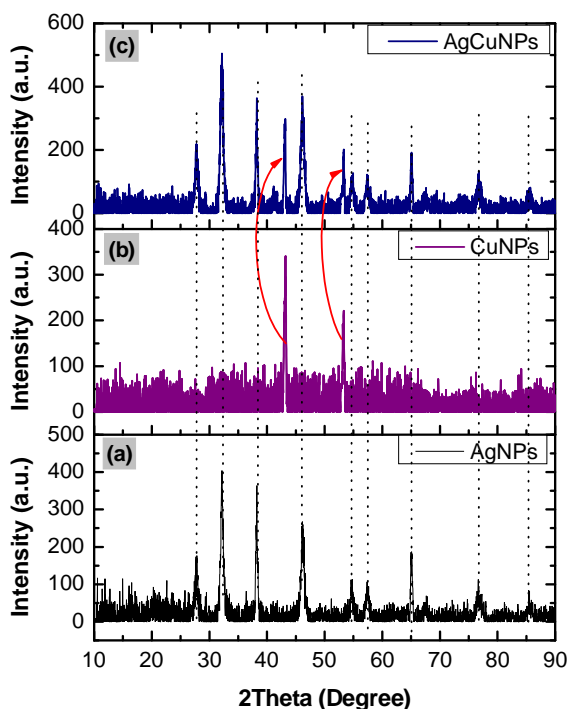
**Table 2.** d spacing value of synthesized AgNPs calculated using  $n=1$  and  $\lambda$  for  $\text{CuK}\alpha=1.5406\text{\AA}$ 

Nanoparticles	Plane	$2\theta$ (in degree)	$\theta$ (in degree)	$d_{hkl} = n\lambda / 2 \sin \theta$ (in $\text{\AA}$ )
AgNPs	111	38.15	19.075	2.36
	220	65.5	32.75	1.423
	311	76.6	38.3	1.24
CuNPs	111	43.06	21.53	2.09
	220	53.36	26.68	1.71
	111	38.15	19.075	2.356
AgCuNPs	111	43.06	21.53	2.098
	220	53.36	26.68	1.714
	220	65.5	32.75	1.423
	311	76.6	38.3	1.242
	110	27.66	13.83	3.22
AgONPs	111	32.16	16.08	2.77
	200	46.14	23.07	1.96
	200	54.56	27.28	1.68
	220	57.28	28.64	1.60
	222	85.16	42.58	1.13

**Table 3.** The grain size of AgNPs, CuNPs, and AgCuNPs calculated based on the intense peak of XRD spectra

Nanoparticles	$2\theta$ (in degree)	$\beta$ (FWHM, in degree)	$\beta = \text{FWHM}$ (rad)	$D = 0.9\lambda / \beta \cos \theta$ (in nm)
AgNPs	38.15	0.732	0.01277	11.81
CuNPs	43.06	0.156	0.00272	55.33
AgCuNPs	38.15 and 43.06	0.693 and 0.15	0.01209	12.45

A comparative study of these three nanoparticles based on their XRD pattern gives more detailed information. This indicated that individual graph peaks resemble the combined bimetallic nanoparticle form indicating the formation of bimetallic nanoparticles.

**Fig. 4.** XRD pattern of a) AgNPs, b) CuNPs, and c) AgCuNPs comparison

### 3.5 Antimicrobial Activities of Nanoparticles

The antimicrobial activities of AgNPs, CuNPs, and Ag-CuNPs synthesized using aqueous extract of *Alternanthera brasiliensis* stem were carried out against Gram-positive bacteria, Gram-negative bacteria, and fungus (*Candida albicans*) as in Figure 5. The antimicrobial properties of each NPs were measured in terms of the zone of inhibition (ZOI). For this experiment, Kanamycin was taken as standard. According to the results, Ag NPs and Ag-Cu NPs had a reduced antibacterial impact on all microorganisms while Cu NPs had a higher zone of inhibition as in Table 4. The antimicrobial activities of Ag-Cu bimetallic nanoparticles are comparatively lower than individual Ag and Cu nanoparticles. This demonstrated the controlled release of the silver and copper ions in the host cells. This control release mechanism is suitably preferred for long-term protection as well. These findings are recommendable and similar to some other research [21, 24].

**Table 4. Zone of inhibition (ZOI) shown by Ag NPs, Cu NPs, and AgCuNPs**

Microorganisms (Test organisms)	List of nanoparticles	ZOI of nanoparticles (cm)	ZOI of Standard Kanamycin (cm)
Bacteria <i>Bacillus subtilis</i> (Gram +ve)	(a) Ag NPs	0.6	0.9
	(b) Cu NPs	0.7	
	(c) Ag-Cu alloy NPs	0.5	
<i>Escherichia coli</i> (Gram -ve)	(a) Ag NPs	0.5	1.0
	(b) Cu NPs	1.0	
	(c) Ag-Cu alloy NPs	0.6	
<i>Candida albicans</i>	(a) Ag NPs	0.5	0.8
	(b) Cu NPs	0.7	
	(c) Ag-Cu alloy NPs	0.5	

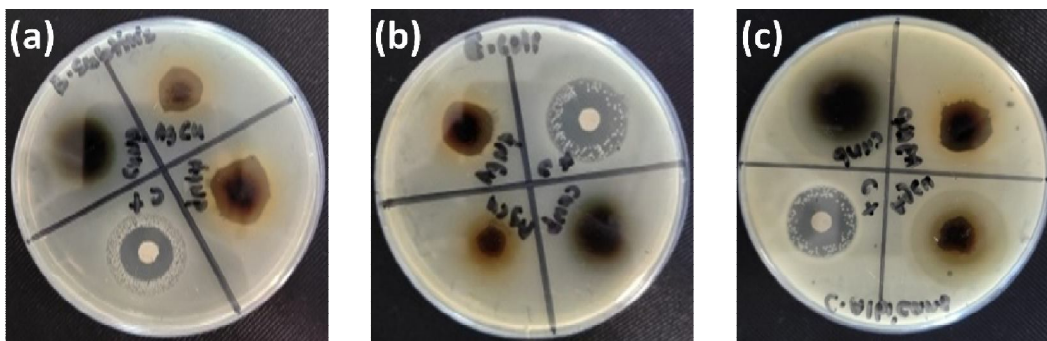


**Fig. 5. Antimicrobial activities of the green synthesized Ag NPs, Cu NPs, and Ag-Cu alloy NPs for a) *Bacillus subtilis*, b) *Escherichia coli*, and c) *Candida albicans***

#### 170 4. CONCLUSIONS

171  
172 Aqueous extract of *Alternanthera brasiliana* stem was used in the study to demonstrate a straightforward and  
173 environmentally benign process for producing silver, copper, and silver-copper bimetallic nanoparticles. Synthesized  
174 nanoparticles were successfully characterized by XRD, FTIR, and UV. UV spectroscopy was employed to observe the  
175 nanoparticle formation, whereas FTIR spectroscopy was used to analyze the reactive groups of the phytochemicals  
176 responsible for nanoparticle stabilization. The stretching aromatic groups C=C conjugated amide groups of C-H and the -  
177 OH, C-O, and -CH<sub>2</sub> were detected in the FTIR spectra. The Debye-Scherrer formula was used to determine the sizes of  
178 silver, copper, and Ag-Cu nanoparticles and was found to be 11.81, 55.33, and 12.45 nm, respectively. Synthesized  
179 AgNPs, CuNPs, and Ag-CuNPs were tested for their antimicrobial properties against fungi (*Candida albicans*) Gram-  
180 positive (*Bacillus subtilis*), and Gram-negative (*Escherichia coli*) bacteria. This implies that the *Alternanthera brasiliana*  
181 stem extract can be suitably used as a capping and reducing agent in the green technique for the synthesis of AgNPs,  
182 CuNPs, and Ag-CuNPs.

#### 183 ACKNOWLEDGMENTS

184  
185 The authors are thankful to the Department of Chemistry, Amrit Campus, and Kathmandu for laboratory support, and  
186 JNCSR, India for XRD measurement.

#### 188 AUTHORS' CONTRIBUTIONS

189  
190 This work was carried out in collaboration among all authors. All authors read and approved the final manuscript.

#### 192 DISCLAIMER (ARTIFICIAL INTELLIGENCE)

193  
194 Author(s) hereby declare that NO generative AI technologies such as Large Language Models (ChatGPT, COPILOT, etc.)  
195 and text-to-image generators have been used during the writing or editing of this manuscript.

#### 197 REFERENCES

- 198 1. Beyene HD, Werkneh AA, Bezabh, HK, Ambaye TG. Synthesis paradigm and applications of silver nanoparticles  
199 (AgNPs), a review. Sustainable materials and technologies. 2017;(13):18-25.
- 200 2. Kalakonda P, Mandal P, Laxmi Mynepally S, Bashipangu A, Kethavath A, Khanam SJ, & Podila BB. Comparison of  
201 multi-metallic nanoparticles-alternative antibacterial agent: understanding the role of their antibacterial  
202 properties. Journal of Inorganic and Organometallic Polymers and Materials. 2024; 34:2203-2218.
- 203 3. Banfield JF, Zhang H. Nanoparticles in the environments. Reviews in Mineralogy and Geochemistry. 2001;44(1):1-58.
- 204 4. Din MI, Rehan R. Synthesis, Characterization, and Applications of Copper Nanoparticles Analytical Letters  
205 2016;50(1):50-62.
- 206 5. Geoprincy G, Srri BV, Poonguzhali U, Gandhi NN, Renganathan S. A review of green synthesis of silver nanoparticles.  
207 Asian Journal of Pharmaceutical and Clinical Research. 2013;6:8.
- 208 6. Rafique M, Sadaf I, Rafique MS, Tahir M. B. A review on green synthesis of silver nanoparticles and their applications.  
209 Artificial cells, nanomedicine, and biotechnology. 2017;45:1272.
- 210 7. Umer A, Naveed S, Ramzan N, Rafique MS. Selection of a suitable method for the synthesis of copper nanoparticles.  
211 Nano. 2012;7:1230005.
- 212 8. Hussain I, Singh N, Singh A, Singh H, Singh S. Green synthesis of nanoparticles and its potential application.  
213 Biotechnology letters. 2016;38:545-560.
- 214 9. Oli HB, Sharma N, Ekaraj K, Subedee A, Timilsina R. Green Synthesis of Copper nanoparticles using Zingiber  
215 officinale Extract and Characterization. Journal of Nepal Chemical Society. 2018;39:10.

- 216 10. Dawadi, S., Katuwal, S., Gupta, A., Lamichhane, U., Thapa, R., Jaisi, S., Lamichhane, G., Bhattarai, D.P., & Parajuli,  
217 N. Current research on silver nanoparticles: synthesis, characterization, and applications. *Journal of*  
218 *nanomaterials*, 2021;1:6687290.
- 219 11. Baruwati B, Polshettiwar V, Varma R. Glutathione promoted expeditious green synthesis of silver nanoparticles in  
220 water using microwaves. *Green chemistry*. 2009;11:926.
- 221 12. Parajuli, S., Nepal, P., Awasthi, G. P., Oli, H. B., Shrestha, R. L. S., Homagai, P. L., & Bhattarai, D. P. Synthesis,  
222 characterization and antimicrobial study of silver nanoparticles using methanolic fraction of *Artemisia vulgaris*  
223 leaf. *BIBECHANA*, 2024;21(1):63–73.
- 224 13. Sharma AK, Rana K, Shrestha S, Oli HB, Bhattarai DP. A comparative Study on Synthesis, Characterization, and  
225 Antibacterial Activity of Green vis-a-vis Chemically Synthesized Silver Nanoparticles. *Amrit Research Journal*.  
226 2022;3:75.
- 227 14. Li S, Shen Y, Xie A, Yu X, Qiu L, Zhang L, Zhang Q. Green synthesis of silver nanoparticles using *Capsicum*  
228 *annuum* L. extract. *Green Chemistry*. 2007;9:852.
- 229 15. Ahmed S, Ahmad M, Swami BL, Ikram S. Green synthesis of silver nanoparticles using *Azadirachta indica* aqueous  
230 leaf extract. *Journal of radiation research and applied sciences*. 2016;9:1.
- 231 16. Bar H, Bhui DK, Sahoo GP, Sarkar P, De SP, Misra A. Green synthesis of silver nanoparticles using seed extract of  
232 *Jatropha curcas*. *Colloids and surfaces A: Physicochemical and engineering aspects*. 2009;339:134.
- 233 17. Shende S, Ingle, AP, Gade, A.; Rai, M. Green synthesis of copper nanoparticles by *Citrus medica* Linn. (Idilimbu) juice  
234 and its antimicrobial activity *World Journal of Microbiology and Biotechnology*. 2015;31:865-873.
- 235 18. Amer M, Awwad A. Green Synthesis of Copper Nanoparticles by *Citrus Limon* Fruits Extract, Characterization and  
236 Antibacterial Activity. *Chemistry International*. 2021;7(1):1-8.
- 237 19. Nagar, N. Devra, V. Green synthesis and characterization of copper nanoparticles using *Azadirachta indica* leaves.  
238 *Materials chemistry and physics*;2018,213:44-51.
- 239 20. Subedee A, Shrestha S, Ghimire S, Pathak I, Oli HB, Sharma AK, Pandey BR, Homagai RL, Shrestha, RL, Bhattarai,  
240 DP. Green Synthesis and Characterization of Copper-Zinc Alloy Nanoparticles Using Stem Extract of *Tinospora*  
241 *cordifolia* and Comparative Study of Anti-Microbial Properties. *Amrit Journal*. 2023;3:78.
- 242 21. Al-Haddad J, Alzaabi F, Pal P, Rambabu K, Banat F. Green synthesis of bimetallic copper–silver nanoparticles and  
243 their application in catalytic and antibacterial activities. *Clean Technologies and Environmental Policy*. 2020;22:269.
- 244 22. Azmat, A.; Zafar, S. *Trigonella foenum-graecum*-based facile one-pot green synthesis, characterization, and biological  
245 activities of silver/copper bimetallic nanoparticles. *Nanotechnology for Environmental Engineering*. 2023;8:733.
- 246 23. Ismail M, Khan M, Khan SA, Qayum M, Khan MA, Anwar Y, Akhtar, Asiri AM, Khan SB. Green synthesis of  
247 antibacterial bimetallic Ag-Cu nanoparticles for catalytic reduction of persistent organic pollutants *Journal of Materials*  
248 *Science: Materials in Electronics*. 2018;29:20840.
- 249 24. Thirumoorthy G, Balasubramanian B, George JA, Nizam A, Nagella P, Srinatha N, Pappuswamy M, Alanazi  
250 AM, Meyyazhagan A, Rengasamy KR. Phytofabricated bimetallic synthesis of silver-copper nanoparticles using *Aerva*  
251 *lanata* extract to evaluate their potential cytotoxic and antimicrobial activities. *Scientific Reports*. 2024;14:1270.
- 252 25. Ragavendran, C., Kamaraj, C., Natarajan, D., Al-Ghanim, K. A., Magesh, M., Nicoletti, M., & Govindarajan, M.  
253 Synthesis of Lawsonia inermis-encased silver–copper bimetallic nanoparticles with antioxidant, antibacterial, and  
254 cytotoxic activity. *Green Processing and Synthesis*, 2024;13(1):20230194.
- 255 26. Thirumoorthy, G., Balasubramanian, B., George, J. A., Nizam, A., Nagella, P., Srinatha, N., Pappuswamy, M., Alanazi,  
256 A.M., Meyyazhagan, A., Rengasamy, K.R.R. & Veerappa Lakshmaiah, V. Phytofabricated bimetallic synthesis of  
257 silver-copper nanoparticles using *Aerva lanata* extract to evaluate their potential cytotoxic and antimicrobial  
258 activities. *Scientific Reports*, 2024;14(1) 1270.

- 259 27. Azmat, A., & Zafar, S. Trigonella foenum-graecum-based facile one-pot green synthesis, characterization, and  
260 biological activities of silver/copper bimetallic nanoparticles. Nanotechnology for Environmental  
261 Engineering, 2023;8(3):733-744.
- 262 28. Muradova, G. G., Gadjieva, S. R., DI PALMA, L., & Vilardi, G. Nitrates removal by bimetallic nanoparticles in water.  
263 Chemical Engineering Transactions, 2016;47:205-210.
- 264 29. Al-Haddad, J., Alzaabi, F., Pal, P., Rambabu, K., & Banat, F. Green synthesis of bimetallic copper–silver nanoparticles  
265 and their application in catalytic and antibacterial activities. Clean Technologies and Environmental  
266 Policy, 2020;22:269-277.
- 267 30. Araya-Hermosilla, R., Martínez, J., Loyola, C. Z., Ramírez, S., Salazar, S., Henry, C. S., Lavin, R. & Silva, N. (2023).  
268 Fast and easy synthesis of silver, copper, and bimetallic nanoparticles on cellulose paper assisted by  
269 ultrasound. Ultrasonics Sonochemistry, 2023;99:106545.
- 270 31. Hao, Z., Wang, M., Cheng, L., Si, M., Feng, Z., & Feng, Z. Synergistic antibacterial mechanism of silver-copper  
271 bimetallic nanoparticles. Frontiers in Bioengineering and Biotechnology, 2024;11:1337543.
- 272 32. Videira, V. D. C. G., Harada, B. N., Vital, V. G., da Silva, R. A. G., de Vasconcellos, S. P., & Pellosi, D. S. Structural  
273 and antibacterial evaluation of copper, silver, and bimetallic silver/copper nanoalloys synthesized in chitosan  
274 biopolymer. Next Materials, 2024;3:100071.
- 275 33. Nazeruddin, G., Prasad, R., Shaikh, Y., & Shaikh, A. Synergetic effect of Ag-Cu bimetallic nanoparticles on  
276 antimicrobial activity. Der Pharmacia Lettre, 2014;3:129-136.
- 277 34. Huston M, DeBella M, DiBella M, Gupta A. Green Synthesis of Nanomaterials. Nanomaterials. 2021; 11(8):2130.
- 278 35. Pereira D, Zanon R, Dos Santos M, Boligon A, Athayde M. Antioxidant activities and triterpenoids isolated  
279 from *Alternanthera brasiliana* (L.) Kuntze leaves. Natural product research. 2013;27:1660.
- 280 36. Nepal, P., Parajuli, S., Awasthi, G. P., Sharma, K. P., Oli, H. B., Shrestha, R. L., & Bhattarai, D. P. Eco-Friendly  
281 Synthesis of CuO@ ZnO Nanocomposites Using Artemisia vulgaris Leaf Extract and Study of Its Photocatalytic Activity  
282 for Methylene Blue. Journal of Nanotechnology, 2024;2024(1):6896986.
- 283 37. Tamilarasi P, Meena P. Green synthesis of silver nanoparticles (Ag NPs) using *Gomphrena globosa* (Globe amaranth)  
284 leaf extract and their characterization. Materials Today: Proceedings. 2020;33:2209.
- 285 38. Sowbaraniya S, Ganesh SB, Rajeshkumar S. Green Synthesis of Copper Nanoparticles Using Stem Extract of *Musa*  
286 *sapientum* and Its Characterization: an in vitro Study. Journal of Pharmaceutical Research International. 2021;33:416.
- 287 39. Silverstein RM, Bassler GC. Spectrometric identification of organic compounds. Journal of Chemical Education.  
288 1962;39:546.
- 289 40. Oli HB, Thapa Magar J, Khadka N, Subedee A. Bhattarai DP, Pant B. *Coriaria nepalensis* Stem Alkaloid as a Green  
290 Inhibitor for Mild Steel Corrosion in 1 M H<sub>2</sub>SO<sub>4</sub> Solution. Electrochem. 2022;3:713.
- 291 41. Thapa Magar J, Budhathoki IK, Rajaure A, Oli HB, Bhattarai DP. Alkaloid Extract of *Ageratina adenophora* Stem as  
292 Green Inhibitor for Mild Steel Corrosion in One Molar Sulfuric Acid Solution. Electrochem. 2023;4:84.
- 293 42. Mehta B, Chhajlani M, Shrivastava B. Green synthesis of silver nanoparticles and their characterization by XRD.  
294 Journal of physics: conference series. 2017;836:012050.
- 295 43. Giri AK, Jena B, Biswal B, Pradhan AK, Arakha M, Acharya S, Acharya L. Green synthesis and characterization of  
296 silver nanoparticles using *Eugenia roxburghii* DC. extract and activity against biofilm-producing bacteria. Scientific  
297 Reports. 2022;12:8383.
- 298 44. Jayarambabu N, Akshaykranth A, Rao TV, Rao KV, Kumar RR. Green synthesis of Cu nanoparticles using *Curcuma*  
299 *longa* extract and their application in antimicrobial activity. Materials Letters. 2020;259:126813.

300 45. Rahman L-u, Shah A, Dionysiou DD, Dodson D, Kay S. Silver–Copper Bimetallic Alloy Nanoscale Electrochemical  
301 Sensor for the Detection of 1,2-Dihydroxybenzene Compounds. *Chemical Education*. 2015;20:1.  
302

303